JOURNAL OF CATALYSIS 157, 482–500 (1995)

Spectroscopic Characterization of Silicalite-1 and Titanium Silicalite-1

Ermanno Astorino,* John B. Peri,* Ronald J. Willey,* and Guido Busca†

*Department of Chemical Engineering, Northeastern University, Boston, Massachusetts 02115; and †Istituto di Chimica, Facoltà di Ingegneria, Università di Genova, I-16129 Genoa, Italy

Received September 8, 1994; revised July 28, 1995; accepted August 4, 1995

Titanium silicalite samples were prepared by two different procedures. A titanium-free sample (silicalite-1) was also prepared. The samples were characterized by XRD, SEM, skeletal FT-FIR and FT-Raman, UV-vis FT-IR of hydroxy- groups and of adsorbed ammonia. The skeletal spectra have been analyzed on the basis of a general interpretation of the vibrational structure of tetrehedra-based silica polymorphs. This lead to a partial modification of the traditional assignments of the skeletal vibrations of zeolites. Framework Ti is found to be responsible for a band near 960 cm^{-1}, in both IR and Raman spectra, and for a shoulder near 510 cm^{-1} in the IR spectra, as well as for other weak perturbations of the silicalite spectra. The two main features have been assigned to the asymmetric stretching and to the rocking modes of Si–O–Ti bridges. Framework Ti is found to act as a Lewis acid center, being able to coordinate ammonia from gas-phase. Extraframework Ti is observed in the form of anatase in samples prepared with the procedure 1 only with Ti content above 2%, while TiO_2 is found in all samples prepared with the procedure 2. Both series of samples are active catalysts of phenol hydroxylation by H_2O_2. © 1995 Academic Press, Inc.

INTRODUCTION

Silicalite-1 is a zeolitic silica polymorph first described by Flanigen *et al.* (1) in 1978, belonging to the so-called MFI topology (2). Silicon can be isomorphously substituted by several other elements in its structure, giving rise to important catalytic materials. Al for silicon substitution gives rise to the ZSM5 zeolite (3) first described by the Mobil group, key material for the so-called MTG (methanol-to-gasoline (4)) process. Ti for Si substitution gives rise to titanium-silicalite (TS1), first described by the ENI group (5), used as the catalyst for phenol hydroxylation with hydrogen peroxide (6) and cyclohexanone ammoximation with H_2O_2 and ammonia (7). Iron, chromium, boron, and vanadium substitution have also been reported, and substitution with two elements as well (8).

The ability of TS1 in activating hydrogen peroxide is certainly related to the particular environment of Ti^{4+} cations in this zeolite. Spectroscopic measurements, like IR (5), Raman (9), UV–visible (10) and EXAFS (11) data, provided information on the nature of titanium sites in TS1. However, the actual environment of Ti ions is still not completely clear. The original interpretation of Taramasso *et al.* (5) assuming Ti in a true substitutional position has been somewhat questioned by Petrini, Zecchina and co-workers (12) suggesting that Si–O–Ti bonds are at least in part hydrolyzed giving rise to SiOH–HOTi structures. On the other hand, it has been shown (13) that the preparation method strongly affects the performances of TS1 samples, some of which are very active and others much less. This could be related to the different local environments of Ti in TS1 samples of different origins, as well as to morphology factors.

In the course of a study concerning the preparation of S1 and TS1 with different procedures (14), we prepared materials that proven to be effective catalysts for phenol hydroxylation by H_2O_2. To have more information on the actual structure of these solids we performed an investigation by IR and Raman spectroscopies, whose results are presented here.

EXPERIMENTAL

(a) *Catalysts Preparation*

The zeolites were prepared according to two different procedures. Procedure 1 was the one according to the method described by Clerici *et al.* (15) at ENI, while procedure 2 was chosen on the basis of those (that apparently slightly differ each other) reported Thangaraj *et al.* (16). In procedure 1, 9.4 g of tetraethyl orthosilicate were mixed with the appropriate amount of titanium(IV) ethoxide and transferred to a Teflon beaker containing 20.3 g of tetrapropylammonium hydroxide. The mixture was heated to 330 K and stirred for 3 h while flushed with nitrogen. The clear gel obtained was then transferred to an autoclave equipped with a Teflon beaker where it was crystallized for 3 days. The crystals were then collected, centrifuged, filtered, dried at 373 K for 1 h, and calcined at 823 K for 5 h. The Ti-free silicalite sample was synthesized in the same way without using the titanium precursor.

0021-9517/95 $12.00

In procedure 2, 9 g of tetraethyl orthosilicate were added to a solution of 14 g of tetrapropylammonium hydroxide. To this solution the appropriate amount of titanium (IV) *n*-butoxide in 4 g of dry isopropyl alcohol was added dropwise under stirring. The resultant solution was stirred for 1 h to complete the hydrolysis. Water was then added and the solution was heated to 348 K for 3 h. The gel was then crystallized like in procedure 1. The crystallization temperature, however, was 438 K. The products were collected, centrifuged, filtered, and dried at 373 K for 1 h. Removal of the template was done by calcination at 823 K for 12 h.

The TS samples prepared with procedure 1 will be hereinafter denoted as TS1E(X) while the samples arising from procedure 2 will be denoted TS1T(X), with X = 100 Ti/Ti + Si (atomic).

(*b*) *Catalyst Characterization*

The X-ray diffraction was performed with a Scintag XDS-2000 X-ray Diffraction System using Cu$K\alpha$ radiation. The samples were run between an angle 2-θ of 18 and 52 with a step size of 0.03°.

SEM micrographs have been taken with a AMR Model 1000 scanning electron microscope instrument. The area of the sample studied was selected using a magnification of 25,000×. Micrographs were taken with an acceleration voltage of 20 kV.

(*c*) *Spectroscopic Measurements*

Skeletal IR spectra have been recorded with a Magna 750 Fourier transform instrument. For the MIR region (above 400 cm^{-1}) KBr pressed disks and beam splitter were used. For the far IR region (FIR, 600-50 cm^{-1}) polyethylene pressed disks and a "solid substrate" beam splitter, along with a polyethylene-DTGS detector, were used.

For surface and adsorption experiments a Perkin–Elmer 1600 FT-IR instrument with conventional heatable IR cells connected to vacuum–gas manipulation apparata were used. The spectra have been recorded using pressed disks of the pure catalyst powders activated by calcination–outgassing in conventional IR cells connected to outgassing–gas manipulation apparata.

The Raman scattering spectra have been recorded with a Brucker FTS100 Fourier transform instrument (Nd-YAG laser).

Diffuse reflectance UV–visible spectra have been recorded on a Varian Cary 5 spectrometer, as reported in Ref. (10).

(*d*) *Catalytic Activity Tests*

Catalytic activity in liquid-phase phenol hydroxylation by H_2O_2 has been investigated in a 250 ml batch reactor at reflux conditions (approx. 353 K) in acetone 20 ml, with 400 mg catalyst, 10 g phenol, and 4 ml H_2O_2 30% in H_2O. Product analysis was performed with a HP 5890 gas chromatograph equipped with a HP1 capillary column (T = 423–453 K, heating rate 30 K/min). Sample size of 1 ml was taken every thirty minutes. This sample was neutralized with 1 ml of a 20 ppm $FeSO_4$ in water solution. Also, 1 ml of acetone was added to the sample mixture in order to create a single miscible phase before injection into the gas chromatograph.

RESULTS

(*a*) *Catalyst Characterization by XRD and SEM*

XRD patterns of the Ti-containing silicalites show the presence of orthorombic MFI-type structures in all cases (5, 17). No other phases are detected by XRD. The XRD pattern of pure S1 additionally shows the splitting of the diffraction peaks near 3.05 and 3.6 Å into two components, according to its well-known monoclinic distortion (17, 18).

SEM micrographs of the samples S1, TS1E(1.25), TS1E(2.5), and TS1T(2.5) are shown in Fig. 1. S1 shows well defined crystallites with a nearly hexagonal prismatic habit, less than 200 nm thick with an area near 1.6×10^5 nm^2. The TS1E crystals all show a more symmetric, nearly cubic-like, well defined shape, their size being slightly smaller for the sample with 1.25% of Ti than for S1, and seems to increase slightly again by increasing Ti content. These habits look similar to those reported in the literature for similar materials (19–21). The samples prepared with procedure 2 have a distinctly different habit, being nearly globular or spherical.

(*b*) *Catalytic Activity in Phenol Hydroxylation*

To compare our materials with those described in the literature we tested them as catalysts for liquid-phase phenol hydroxylation with H_2O_2 in acetone. The results of these experiments are described in Table 1. As expected, pure S1 is catalytically inactive while the Ti-containing samples show a behaviour similar to that of good catalysts reported in the literature (6, 19), although the shift in selectivity towards catechol at the expense of hydroquinone seems to be an exception. Conversion versus time data supported a first order reaction in phenol concentration for all samples. The resultant intrinsic first order rate constant (per hour per gram of catalyst) is also reported in Table 1.

The catalytic activity of the samples prepared with procedure 1 increases with Ti content up to 2.5%, and later decreases. In contrast, the catalytic activity of the samples prepared with procedure 2 increases up to Ti content 2.5% but later it levels off. The sample TS1E(2.5) is the most active with cathechol yields of near 20% and an intrinsic first order rate constant of 0.186 h^{-1} per g of catalyst.

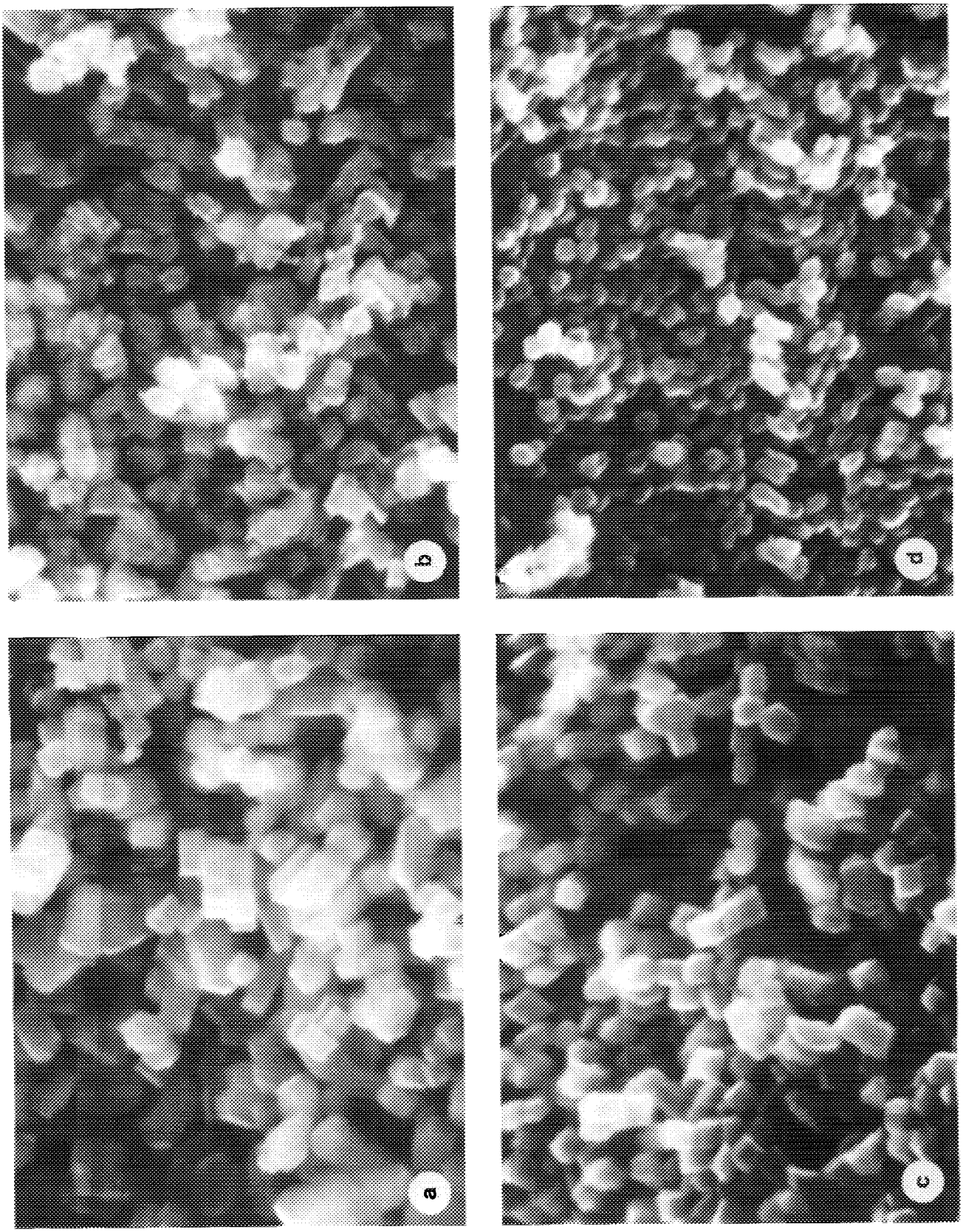

FIG. 1. SEM micrographs of S1 (a), TS1E(1.25) (b), TS1E(2.5) (c), and TS1T(2.5) (d). Magnification ×23,500.

TABLE 1

Phenol Conversion and Product Selectivities in Liquid Phase Phenol Hydroxylation by H_2O_2 after 3 h at 353 K (Reflux)

Zeolite	Phenol conversion %	First order rate constant $k(h^{-1} g^{-1})$	Selectivities			
			ortho %	*meta* %	*para* %	benzoquinone %
S1	0.0	=	0.0	0	0	0
TS1E(1.25)	6.0	0.036	100.0	0	0	0
TS1E(1.80)	14.9	0.122	100.0	0	0	0
TS1E(2.5)	24.0	0.186	83.2	0	16.8	0
TS1E(5)	15.2	0.132	92.3	0	7.7	0
TS1E(10)	8.7	0.069	100.0	0	0	0
TS1T(1.35)	8.9	0.076	100.0	0	0	0
TS1T(2.5)	16.7	0.139	91.1	0	8.9	0
TS1T(5)	18.1	0.156	87.5	0	12.5	0
TS1T(7.5)	17.8	0.156	94.2	0	5.8	0
TS1T(10)	17.1	0.153	91.5	0	8.5	0

Note. ortho = cathechol; *meta* = resorcinol; *para* = hydroquinone.

(c) *Skeletal IR and Raman Spectra*

The IR skeletal spectrum of pure S1 (Fig. 2, bottom) agrees with those reported in the literature (5, 11, 21) showing five prominent features, although all are clearly multiple. The main maxima are observed at 1232, 1104, 804, 552, and 447 cm^{-1}. However, two weaker individual maxima are detectable at 628 and 588 cm^{-1} and shoulders are evident near 1170 (broad), near 960 (very weak), 820, 790, 600, 562, 545, 495, 420, 400, 375, and 350 cm^{-1}. The IR spectrum of the sample TS1E(1.25) (Fig. 2, top) is closely related to that of S1 although a well resolved medium-strong individual maximum at 955 cm^{-1} is additionally present. Moreover, the overall spectrum is apparently

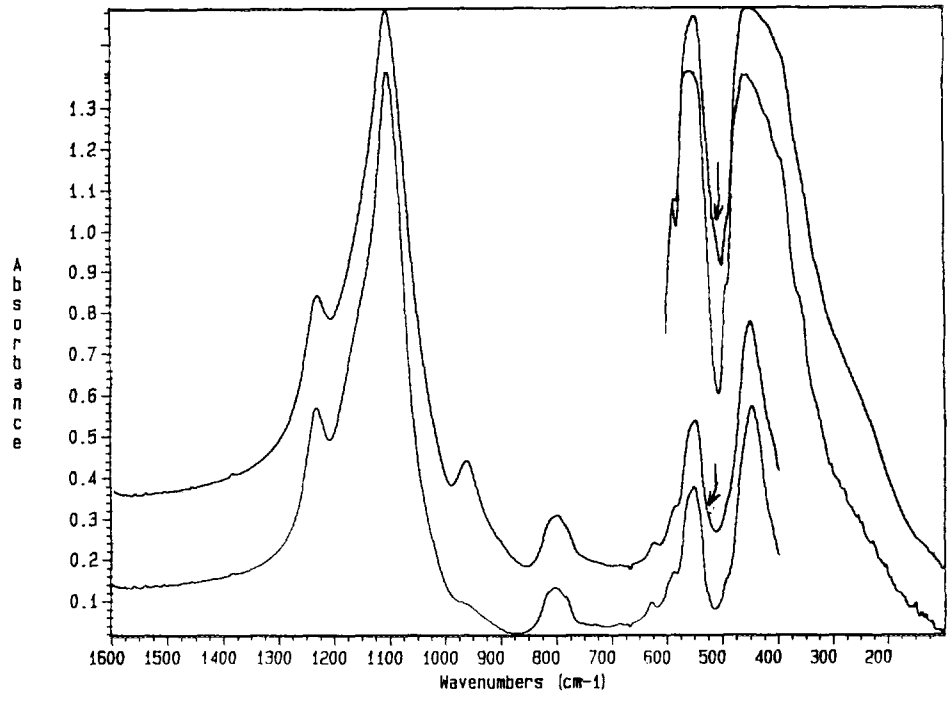

FIG. 2. FT-IR/FT-FIR spectra of S1 (bottom) and TS1E(1.25) (top). The arrows mark a shoulder in the TS1 spectrum (see text).

slightly less resolved. Further addition of titanium (procedure 1) does not cause any other clear effect on the IR spectra except the apparent increase of the relative intensity of the maximum near 450 cm $^{-1}$ with respect to that near 550 cm $^{-1}$ and the increase of the absorption at the minima near 500 and 700 cm $^{-1}$ (Fig. 3). When Ti content rises 5% a shoulder is also observed near 250 cm^{-1}.

Additional information can be obtained by analysing the subtraction spectra (Fig. 4). The subtraction spectrum TS1 − S1 besides showing the formation of the above cited prominent band measured in the subtraction spectrum at 950 cm^{-1}, provides evidence for components growing at the lower frequency side of the strongest bands in the region 1300–1000 cm^{-1}, namely near 1200, 1125, and 1040 cm $^{-1}$. Also the complex band centered near 800 cm $^{-1}$ is partly shifted down while at lower frequency many negative and positive small peaks evidence the existence of a great number of weak components that are perturbed by Ti addition. One of them, evident as a positive band near 515 cm $^{-1}$, is particularly strong. This feature corresponds to a shoulder distinguishable in the spectrum of TS1, although being located near a minimum in absorption between the 550 and 450 cm $^{-1}$ bands (see arrows in Fig. 2, top).

The subtraction spectra with other higher Ti-content samples confirm the following information:

(i) The strongest bands in the region 1300–1000 cm^{-1} are all slightly shifted downwards by Ti addition; (ii) the mode typical of TS samples at 950 cm $^{-1}$ grows further slightly; (iii) a great number of components is detectable below 900 cm^{-1}; (iv) a relatively strong component is formed near 515 cm^{-1}. Moreover, the increase of the absorption in the region below 900 cm^{-1} (evident looking at the absorbance at the minima near 500 and 700 cm^{-1} and the relative absorbance at the maxima near 550 and 450 cm^{-1}) is actually due to the growth of a broader spectrum centered in the typical absorption region of TiO_2 polymorphs (anatase and rutile (22)), as shown in Fig. 4, top.

The IR spectra of the TS samples prepared with the procedure 2 (Fig. 5) are similar to those prepared with procedure 1, although one can have the suspect that the TiO_2 spectrum is already present in the case of TS1T(1.35). However, it seems interesting to remark that the IR spectra of the TS1 materials reported by Thangaraj *et al.* (16) differ from ours and from those reported in the other literature, because they present an additional medium strong band near 750 cm^{-1}. So, it seems evident that the materials studied by Thangaraj *et al.* (16) either present impurities or

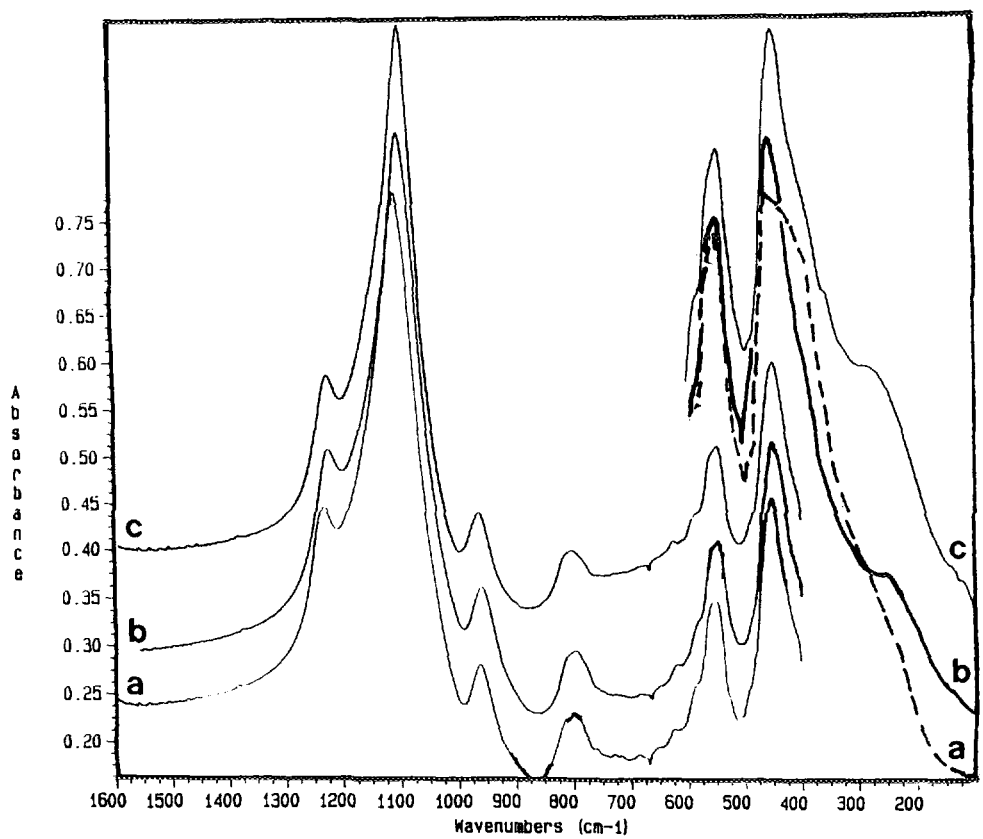

Fig. 3. FT-IR/FT-FIR spectra of the samples (a) TS1E(2.5), (b) TS1E(5), and (c) TS1E(10).

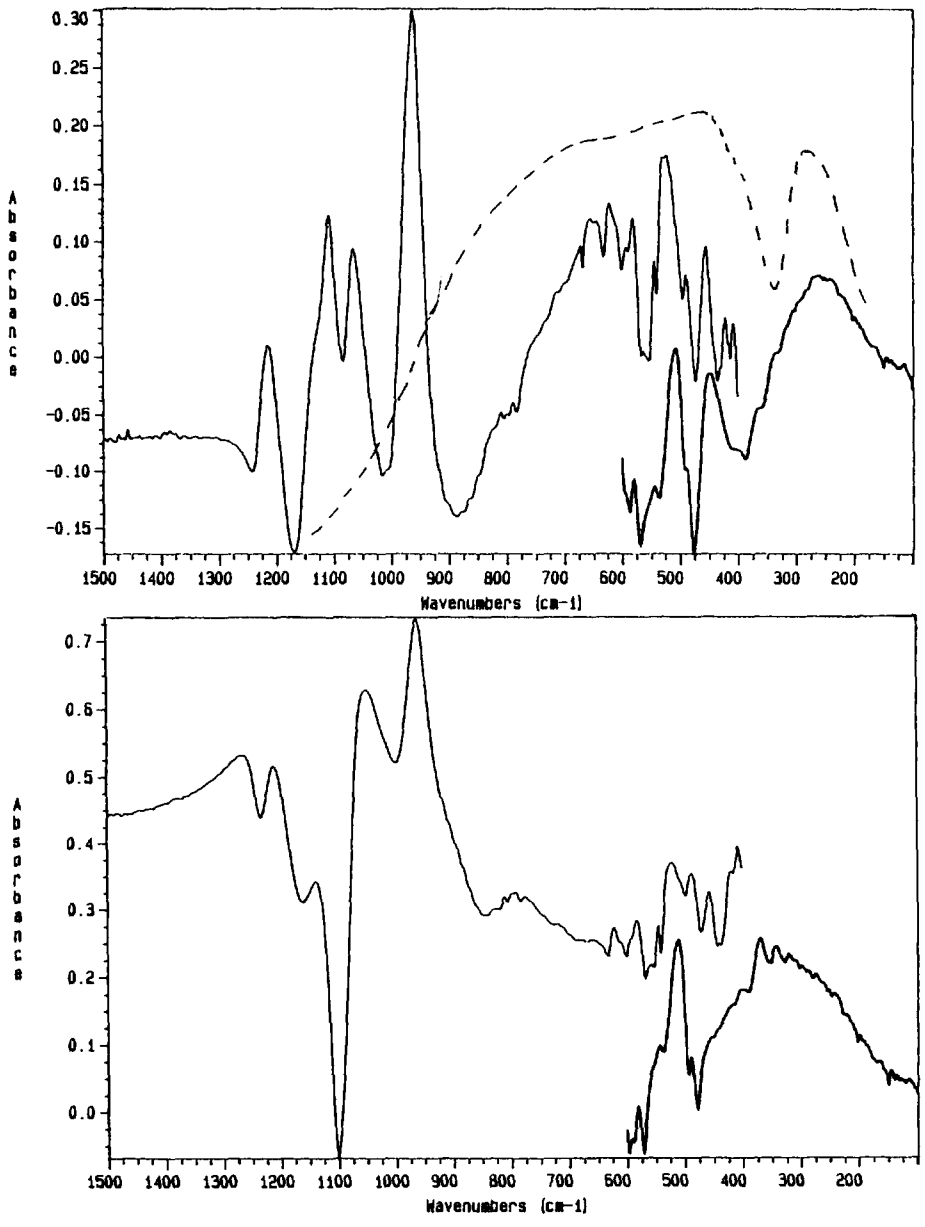

FIG. 4. Subtractions of FT-IR/FT-FIR spectra. Bottom: TS1E(1.25)-S1. Top: TS1E(10)-S1. Broken line: TiO_2-anatase.

contain a different phase than ours and typical silicalites and TS1 materials.

The FT-Raman spectrum of silicalite S1 (Fig. 6, bottom) also agrees with those reported in the literature (12, 23, 24). It is mainly characterized by a strong peak split at 380 cm^{-1} (main maximum) and 365 cm^{-1} (shoulder) and by a number of much weaker maxima: they are observed near 1230, 1095, 975 cm^{-1} in the higher frequency region, together with a complex of weak absorptions at 835, 820, 803, and 790 cm^{-1}, and with individual components at 473, 450, and 435 cm^{-1} in the lower frequency region. The Raman spectrum of titanium silicalite TS1E(1.25) (Fig. 6, top) is virtually identical to that of S1 except for a prominent peak well evident at 970 cm^{-1}. The sample TS1E(2.5) (Fig. 7, bottom) shows additional maxima at 638 and 145 cm^{-1}, that correspond to the two strongest Raman peaks of TiO_2-anatase (22, 24). At higher Ti loadings (preparation 1) the complete pattern of TiO_2-anatase is found, with sharp peaks at 639, 516, 395, 196 and 146 cm^{-1} (Fig. 7).

The FT-Raman spectra of the TS samples prepared with the procedure 2 (Fig. 8) clearly show the anatase pattern already at 1.35% Ti content, and, for similar Ti loadings, stronger anatase peaks than the corresponding samples prepared with the procedure 1.

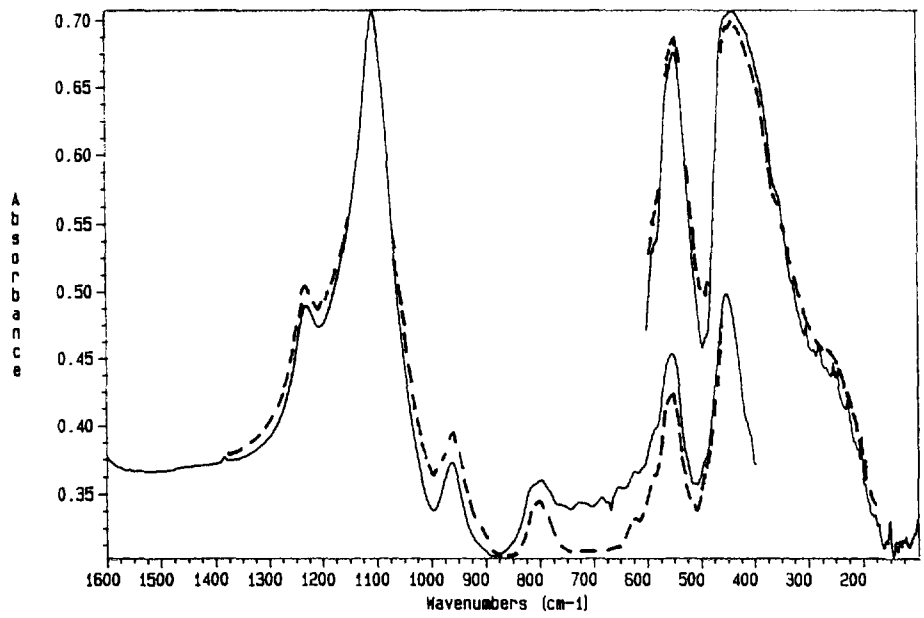

FIG. 5. FT-IR/FT-FIR spectra of the samples TS1T (1.35) (broken line) and TS1T (2.5) (full line).

The comparison of the intensities of the Raman patterns of Figs. 6–8 emphasizes the strength of the TiO_2 Raman peaks as compared to the weakness of silicalite Raman peaks. This makes Raman spectroscopy a very powerful tool for the detection of TiO_2 in TS1 preparations.

(*d*) *Diffuse Reflectance UV–Visible Spectra*

The IR and Raman spectra discussed above show that framework Ti is present in all TS1 samples. However, Raman spectra indicate that TiO_2-anatase is also always present except in TS1E(1.25) that should consequently be a pure Ti-silicalite sample. To verify this conclusion, we also investigated this sample together with all others of the TS1E series by UV–vis spectroscopy, that is sensitive to extraframework Ti similarly as or even more than Raman spectroscopy (10). The DR-UV-vis spectra of S1, TS1E(1.25) and TS1E(2.5) and of a pure TiO_2 (anatase) sample are shown in Fig. 9. The sample S1 only shows in the region 50,000–30,000 cm^{-1} a weak tail associated to

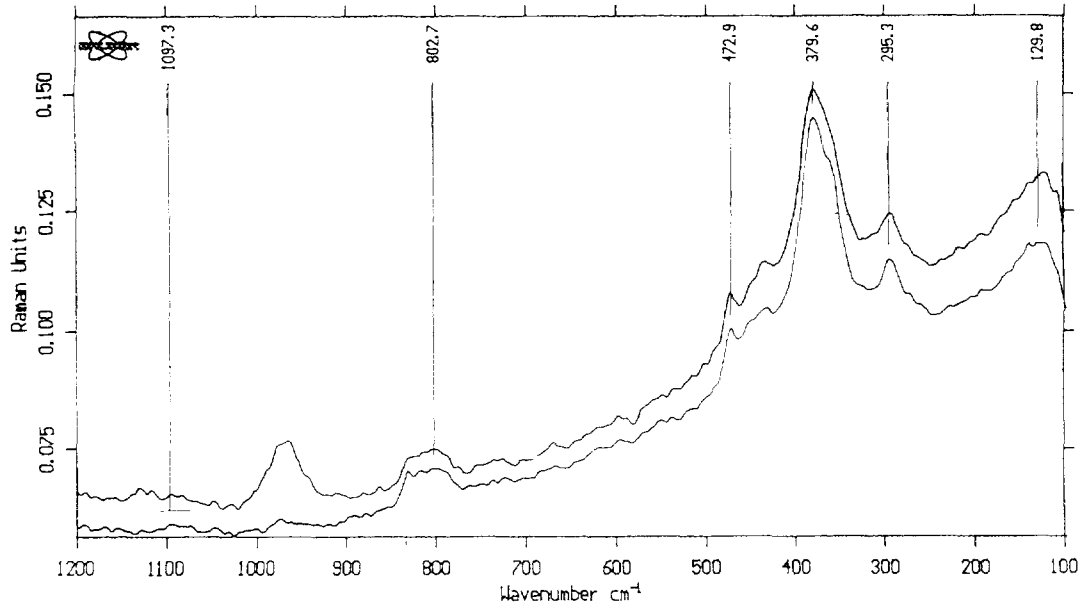

FIG. 6. FT-Raman spectra of S1 (bottom) and TS1E (1.25) (top). Raman units are arbitrary units of light intensity.

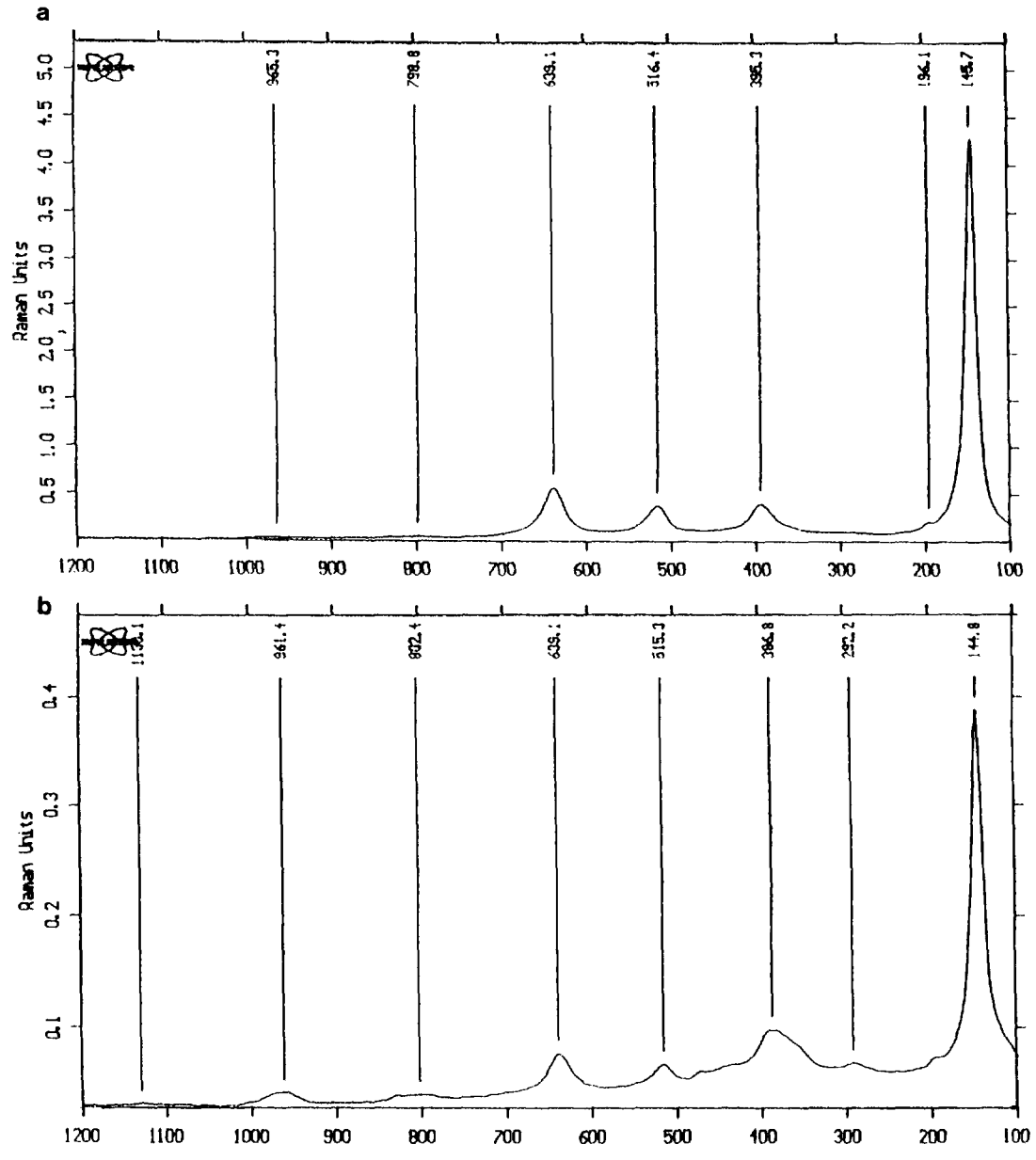

FIG. 7. FT-Raman spectra of the samples (a) TS1E(2.5), (b) TS1E (5), and (c) TS1E (10). Raman units are arbitrary units of light intensity.

the onset of the edge due to the valence band→ conduction band transition. The TiO_2 sample shows instead a strong edge centered at 27,800 cm^{-1} (onset at 24,000 cm^{-1}) assigned to a $O^{2-} \rightarrow Ti^{4+}$ charge transfer transition, corresponding to the valence band → conduction band transition, in the structure where Ti is octahedrally-coordinated.

The spectra of both TS1E(2.5) and TS1E(1.25) are dominated by a strong absorption whose maximum is near 48,000 cm^{-1}, previously assigned to a $O^{2-} \rightarrow Ti^{4+}$ charge transfer transition of tetrahedrally coordinated Ti in the silicalite framework, typical of Ti silicalites (10).

The edge of anatase near 27,800 cm^{-1} is also present, weak, in the spectrum of TS1E(2.5) confirming the presence of anatase-like particles in this sample while for TS1E(1.25) only a broad tail is detectable in the range 27,000–40,000 cm^{-1}, and can be associated to small amounts of extraframework Ti species, likely in an almost amorphous form (10). The overall spectrum of TS1E(1.25) is closely similar to that reported by Geobaldo *et al.* (10) for "well manufactured Ti silicalite." Consequently, UV–vis spectra and Raman spectra confirm each other showing that TS1E(1.25) is almost pure

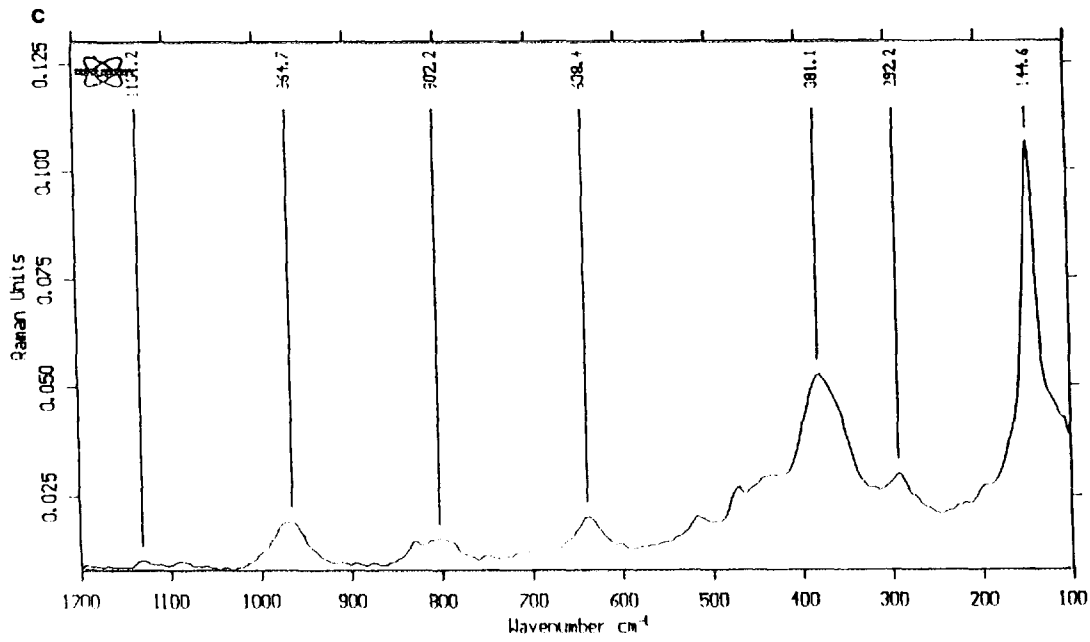

FIG. 7—*Continued*

Ti-silicalite while all other TS1 samples are impure of anatase.

(*e*) *FT-IR Spectra of Surface Hydroxy-Groups*

In Fig. 10 the FT-IR spectra of the surface hydroxy groups of silicalite S1 and of the anatase-free titanium silicalite sample TS1E(1.25) are compared. After activation in vacuum at 773 K the S1 sample shows a sharp band at 3733 cm^{-1} together with a second broader band centered near 3510 cm^{-1}. However, in between, shoulders can be found centered near 3680 and 3625 cm^{-1}.

In Fig. 10 the spectrum of the S1 after contact with few Torrs of water vapour and a brief outgassing at r.t. is also reported. It shows a broad strong band in the region 3500–3000 cm^{-1} associated to H-bonded OHs of water molecules and of silanol groups. A small amount of silanols free from H-bonding is present in these conditions, and is responsible for the residual sharp band at 3735 cm^{-1}. However, in these conditions it is very evident also the component near 3680 cm^{-1}, due to OHs that are not involved in bonding with water, but are different from "normal" free silanol groups. This feature, present also in the spectrum of TS1, coincides with a band frequently associated to extraframework alumina in the ZSM5 zeolite. However, in our case the impurity Al content is certainly very small, if any, and no evidence can be found of alumina particles.

After the same pretreatment the TS sample shows similar components but the broad band at lower frequencies (3510 cm^{-1}) is by far weaker. If the S1 sample is activated at 873 K its hydroxy-group spectrum is similar to that of the TS1 sample activated at 773 K.

This indicates that Ti ions do not give an evident contribution to the OH group spectra. On the other hand, it has been shown before, working with SiO_2–TiO_2 mixed oxides, that the intensity of the OH stretchings of TiOH groups is by far weaker than that of SiOH groups (25). Moreover, the Ti content in sample TS1E (1.25), thought to be entirely in framework position, is small.

The overall structure of the OH stretching region in our silicalite sample looks very similar to that reported for high-silica ZSM5 by Dessau *et al.* (26) and to that studied in detail by Zecchina *et al.* (27), who were able to assign five different components to different OH structures.

The higher frequency sharp band, typical of all silica-containing materials, is associated to "normal" H-bonding-free silanol groups, although its position at slightly lower frequencies with respect to those typical of amorphous silica (3735 *vs* 3747 cm^{-1}) has been attributed to the location of the silanol group internal to the zeolite pores (27). However, the complete absence of external silanols is somewhat surprising. The components near 3680 and 3620 cm^{-1} have been assigned by Zecchina *et al.* (27) to different structures of "terminal" OH groups (i.e., whose oxygen atom only is involved in hydrogen-bonding) into zeolitic pores. However, we think that the component near 3620 cm^{-1} could be assigned, alternatively, to acidic OHs associated to Al impurities, like in ZSM5 zeolites (28).

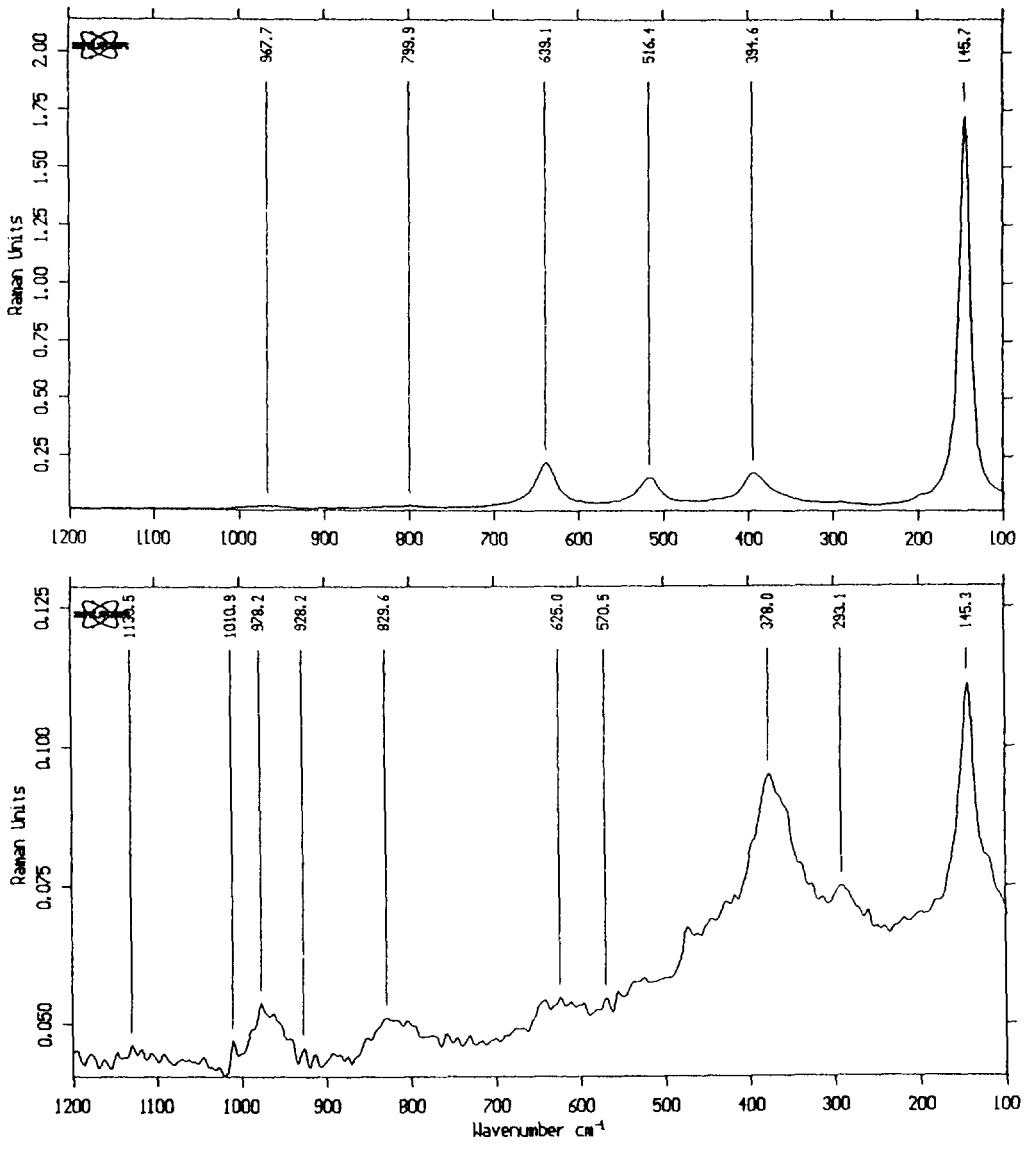

FIG. 8. FT-Raman spectra of the samples TS1T(1.35) (bottom) and TS1T(2.5) (top). Raman units are arbitrary units of light intensity.

The band near 3510 cm^{-1}, strong in the S1 spectrum, is very weak but present also in the TS1 spectrum. According again to Zecchina *et al.* (27), it seems likely that such a band is associated to H-bonded OHs, possibly due to defects in the silicalite structure. Interestingly, in our spectra these defects appear to be more abundant or more stable in the S1 sample than in the TS1 sample.

In effect, according to Scarano *et al.* (12), silicalite can contain a different amount of such defects, likely localized mainly in internal pores. We can conclude from the analysis of the OH stretching region that:

(i) our silicalite sample is rich in defects, more than the titanium silicalite sample TS1E(1.25).

(ii) our samples, also from the point of view of the surface structure, definitely correspond to those described in the literature by the groups of Clerici and Bellussi (15, 19) and of Zecchina and Petrini (27) and by the Mobil group (26).

(iii) Ti–OH groups, if any, cannot very likely be evidenced because of the intrinsic weakness of their IR bands and their poor abundance.

(*f*) *FT-IR Study of Ammonia Adsorption on S1 and TS1*

In Fig. 11 the spectra of a pressed disk of the TS1E(1.25) sample, after activation at 773 K and after ammonia adsorption are reported. In the region 2500–1400 cm^{-1} a number of medium-strong bands associated to overtones

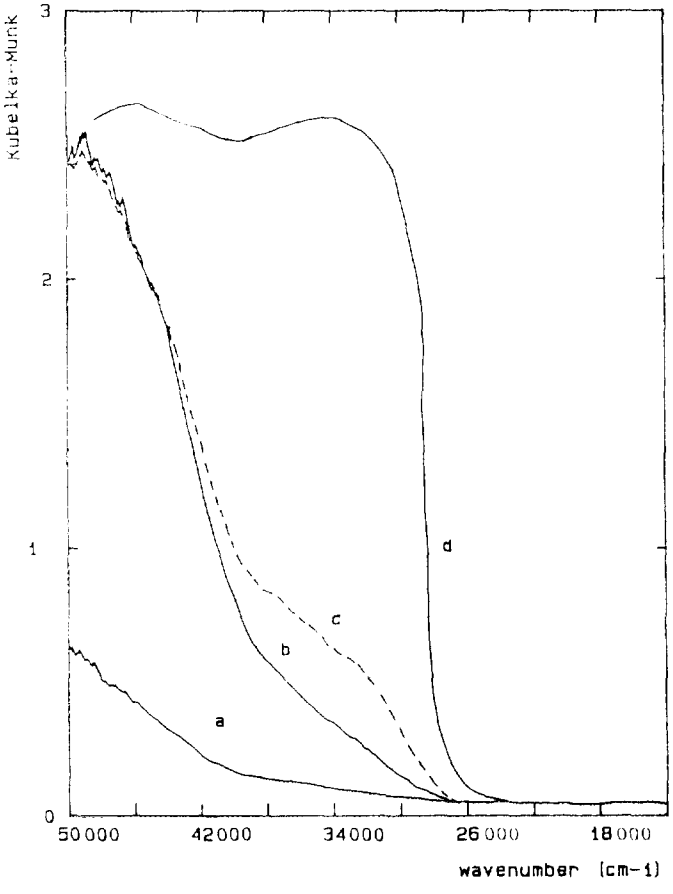

FIG. 9. DR-UV–vis spectra of S1 (a), TS1E(1.25) (b), TS1E(2.5) (c), and of a pure TiO2 (anatase) sample (d).

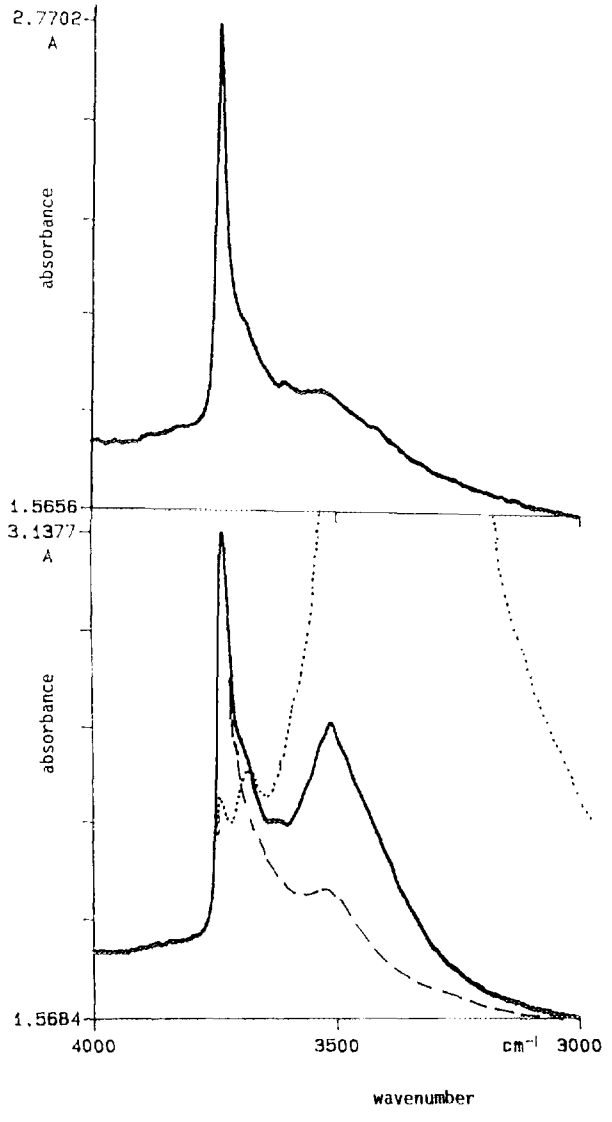

FIG. 10. FT-IR spectra of the surface hydroxy-groups of S1 (bottom) outgassed at 300 K (point line), 773 K (full line) and 873 K (broken line) and of TS1E(1.25) outgassed at 773 K (top).

of the fundamental lattice modes are observed, as on S1 and amorphous silica. No relevant difference is found between the spectra of TS1 and S1 in this region. In contact with 20 Torr of ammonia, the band of free silanol groups at 3735 cm^{-1} is strongly decreased in intensity, while a strong broad band is found, centered near 3000 cm^{-1}, due to the OH stretchings of silanol groups H-bonded to ammonia. Adsorbed ammonia species are responsible for the sharp band at 3395 cm^{-1} (asymmetric NH_3 stretching). However, a definite band is also observed at 1485 cm^{-1}, due to the asymmetric NH_4 deformation mode of ammonium ions. Another interesting feature is that the transmittance of the disk increases in the region below 1400 cm^{-1} upon ammonia adsorption.

After outgassing at r.t. the band of the free SiOH groups is completely restored, as also shown the subtraction spectrum. However, in these conditions, bands at 3395, 3295 and near 1600 cm^{-1} show that adsorbed ammonia species are still present. Interestingly, the last feature is clearly split into two components, at 1635 cm^{-1}, shoulder, and at 1608 cm^{-1}, main maximum (see insert in Fig. 10). Traces of ammonium ions are possibly still present while a negative band is clearly evident in the subtraction spectrum centered at 1370 cm^{-1}, corresponding to the lowering in absorption of TS1 upon ammonia adsorption, cited above. This feature clearly indicates that a surface-sensitive mode is present in this region. Moreover, two broad bands are detectable at 2800 and 2350 cm^{-1}. These features, due to the Fermi resonance between the OH stretching and the first overtone of the in-plane deformation of H-bonded silanols, are typical of almost symmetric H-bondings, where the proton is partially transferred from the OH to the basic molecule (29), ammonia in this case. This indicates that some very acidic silanol groups are still interacting with ammonia molecules.

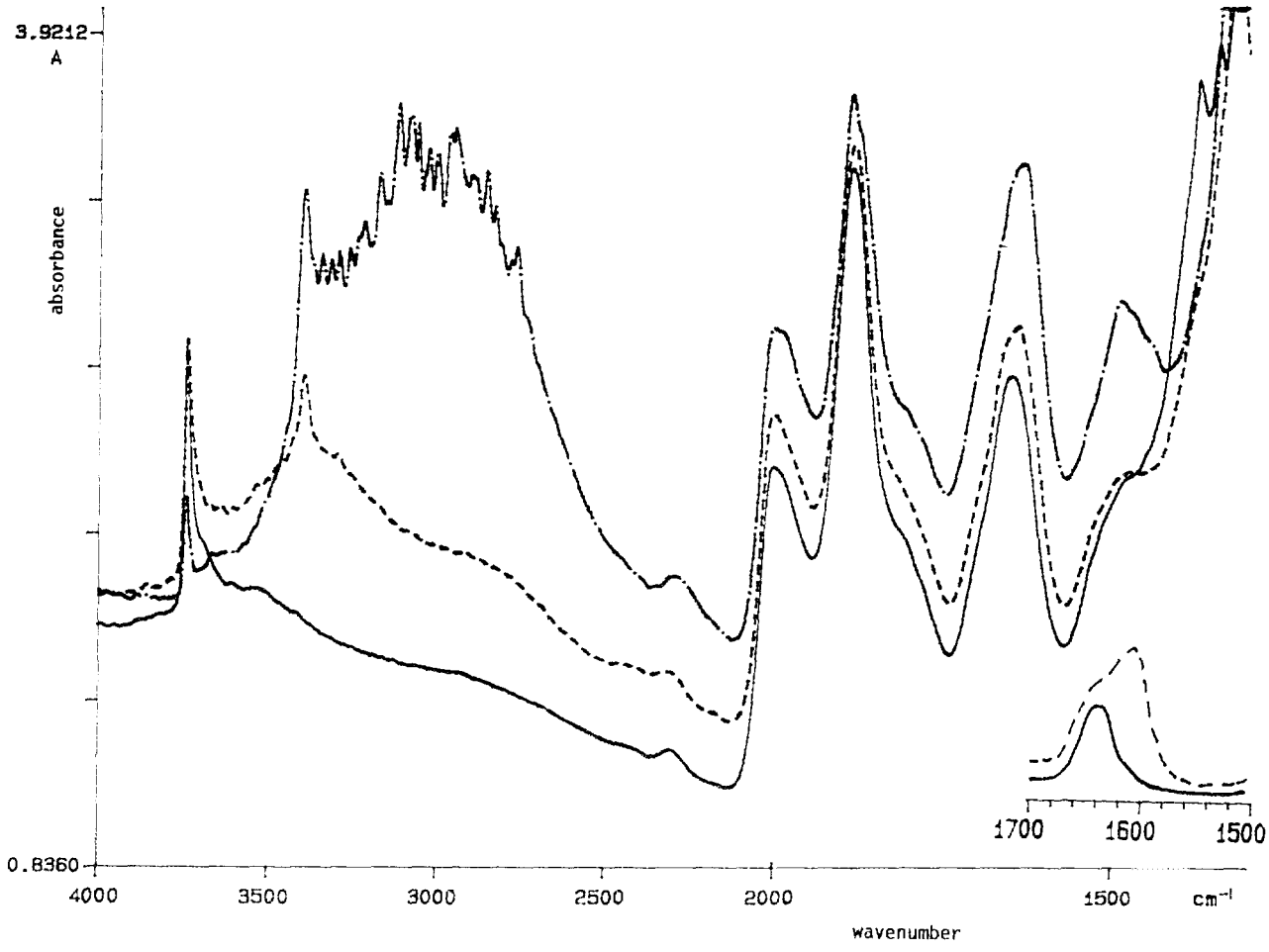

FIG. 11. FT-IR spectra of TS1E(1.25) activated at 773 K (full line), in contact with ammonia 10 Torr (dashed line) and outgassed at 300 K (broken line). In the insert: subtraction spectra relative to ammonia adsorbed on S1 (full line) and on TS1E(1.25) (broken line) after outgassing at 300 K, asymmetric deformation region.

The same experiment has also been performed over pure silicalite S1 (Fig. 12). The spectra gave similar results, but with a main difference: the H-bonded species are apparently more stable on pure silicalite than on TS. They are in fact still abundant after outgassing at 300 K. However, other subtle but very remarkable differences can be found. The asymmetric deformation mode of adsorbed ammonia is on silicalite a simple sharp band centered at 1638 cm^{-1}, in contrast to the evident splitting with an additional predominant component at 1608 cm^{-1} found on TS1 (see insert in Fig. 11). Moreover, the more intense N–H stretching band is found at slightly higher frequencies on S1 (3400 cm^{-1}) than on TS1 (3395 cm^{-1}). Finally, the ratio of the intensities of the ammonia bands (namely that at 3395 cm^{-1}) with repect to the broad component near 3000 cm^{-1} is always stronger on TS1 than on S1.

Previous studies of ammonia physisorbed on amorphous silica gave similar results than on silicalite, with bands of adsorbed ammonia at 3402, 3319, and 1635 cm^{-1} (30). In contrast, ammonia coordinated on Lewis acid sites, like on TiO_2 (31), typically shows all these modes shifted to lower frequencies, the asymmetric deformation mode being detected below 1610 cm^{-1}. These data provide evidence of different adsorbing sites on TS1 with respect to S1, and, in particular, of the presence of Lewis acid sites on TS1. Ammonia species responsible for bands at 3395, 3295, and 1608 cm^{-1}, present only on TS1, must in fact be identified as species interacting with Lewis acid sites, while species absorbing near 3400 cm^{-1} and at 1635 cm^{-1}, present on both S1 and TS1 are certainly H-bonded to silanol groups. This leads to an unequivocal evidence for the presence on our TS1 sample of Lewis sites, reasonably identified as framework Ti cations.

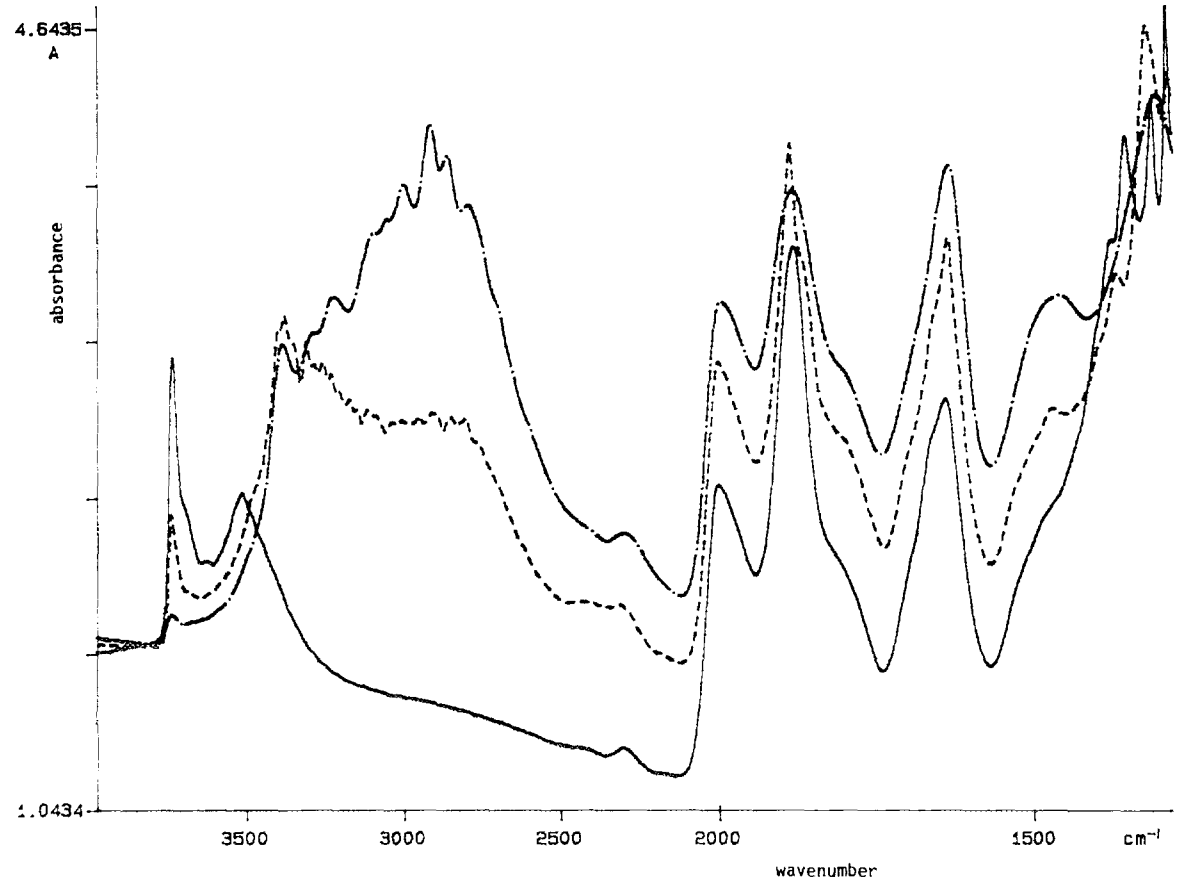

FIG. 12. FT-IR spectra of S1 activated at 773 K (full line), in contact with ammonia 10 Torr (dashed line), and outgassed at 300 K (broken line).

DISCUSSION

(*a*) *Interpretation of the Vibrational Spectra of Silicalite and Other Silica Polymorphs*

Silicalite belongs to the $P2_1/n = C_{2h}^5$ monoclinic space group (No. 14) with $Z = 96$ (1, 18). It transforms into an orthorhombic structure, belonging to the Pnma $= D_{2h}^{16}$ space group (n. 62) between 350 and 363 K. Substituted silicalites like ZSM5 zeolite (3) and Ti-silicalite (5, 17) take the orthorhombic structure already at r.t., the transition temperature being strongly shifted at lower temperatures.

The factor group analysis (32) for monoclinic silicalite gives the following irreducible representation for the optical modes:

$$\Gamma_{opt} = 216\,A_g\,(R) + 216\,B_g\,(R) + 215\,A_u\,(IR) + 214\,B_u(IR).$$

For the orthorhombic structure the following irreducible representation is obtained:

$$\Gamma_{opt} = 110\,A_g\,(R) + 106\,B_{1g}\,(R) + 110\,B_{2g}\,(R) + 106\,B_{3g}\,(R) + 106\,A_u\,(\text{inactive}) + 109\,B_{1u}\,(IR) + 105\,B_{2u}\,(IR) + 109\,B_{3u}\,(IR).$$

Accordingly, 429 IR active modes and 432 Raman active modes are expected for the monoclinic structure and 323 IR active modes and 432 Raman active modes are expected for the orthorhombic form. It is evident that the experimental spectra show much less components, because of the superimposition of much of them. This has also been found for several zeolites with big unit cell dimensions.

As already remarked, silicalite is virtually pure SiO_2, so being a new polymorph of silica with tetrahedrally coordinated silicon, together with α- and β-quartz, α- and β-cristobalite, tridimites, coesite, and moganite. So, its vibrational structure can be discussed in relation to those of these other silica forms, as well as to that of amorphous or vitreous silica (33, 34). The position of the observed vibrational modes of silicalite is compared in Table 2 with that observed for other silica polymorphs and for amorphous silica. However, the interpretation of the vibrational

TABLE 2

Densities (d, g/cm^3) and Position of the Most Intense Vibrational Peaks (cm^{-1}) in the IR and Raman Spectra of Different Silica Forms

	Silicalite		α-Tridimite		α-Cristobalite		α-Quartz		Coesite		Amorphous SiO_2	
d	1.76 IR	2.28 Raman	IR	2.33 Raman	IR	2.65 Raman	IR	2.91 Raman	IR	— Raman	IR	Raman
Mode												
$\nu 1''$	1232	1230	1219		1197	1193		1235	1220		1208	1200
	1170		1145		1160		1166	1162	1160	1164		
										1144		
$\nu 1'$	1104	1095	1108		1096	1076	1086	1085	1085	1065	1100	1060
			1073					1069	1040	1036		
SiOH	960	975									950	970
		835							837	837		
	810	820	820					808	814	815		
$\nu 2$	807	803	795		798	796	798	796	795	785	805	800
	790	790				785	778	778				
							694	696	683			
	600								600			608[a]
	562		585		624				560			
	552		541		525		511	511			560	
	545											490[a]
	495	473						495	490		466	
$\nu 3$	447	450	485		493		461	(464)	435	425	465	
	420	435						450				
	375											
	350											
				457								
				449								
				422		421		465		521		430
$\nu 4$		380		403				401		466		
		365			385		397	394	390	427		
			338				373	365	340	355		
			309		298			355		326		
			279				263	265		269		
						230		206		204		
lattice										176		
										151		
					146	110		128		116		
Refs.	t.w.	t.w.	33	34	33	34,36	t.w.	34	36	41	t.w.	38

[a] Defect bands.

spectra of such SiO_2 forms is still uncomplete and somewhat under debate (33–36). Moreover, most of the published literature on the vibrational structure of silica polymorphs is limited by the use of one only of the two complementary vibrational techniques, IR and Raman. Recently, lattice dynamics calculations have been performed on α-quartz and on zeolitic silica frameworks (assumed to be Al-free) by Van Santen *et al.* (37). These calculations proven to be quite reliable to predict the IR and Raman spectra of silica-like frameworks, although they allow with some difficulty the interpretation of the origin of the different observed peaks and the comparison among different structures. An empyrical interpretation of the spectra of SiO_2 polymorphs will be attempted here, thought to be of simpler use (although, obviously, far less rigorous).

The IR spectra of all tetrahedral silica polymorphs have bands in three regions, i.e., in the region 1300–950 cm^{-1} (very strong, hereinafter denoted $\nu 1$), 850–600 cm^{-1} (medium strength, $\nu 2$) and near 450 cm^{-1} (very strong, $\nu 3$). Raman spectra show very weak peaks in the 1300–950 cm^{-1} and 850–700 cm^{-1} regions ($\nu 1$ and $\nu 2$ modes), and

one or more very strong peaks below 550 cm^{-1}, in a position very sensitive to the overall crystal structure of the solid ($\nu 4$). These features are also present in the spectra of amorphous or vitreous silica; so they contain vibrations of the basic structural units of both crystalline and amorphous silica, i.e., SiO_4 tetrahedra and bridging oxygens. Additional sharp peaks can be found in the IR and Raman spectra of crystalline polymorphs in the region below 700 cm^{-1}, and are certainly associated with splittings of the above modes, due to crystal structure effects, and to torsional lattice modes.

The interpretation of the spectra of silica polymorphs can be attempted on the basis of a model assuming the bridging Si_2O (or T–O–T) "molecule" as a monomeric unit, as done by Bell and Dean (38) and by Galeener (39) for amorphous silica. This approach, we will apply to our materials, gives rise to a somewhat different assignment of the skeletal bands with respect to that of the model first proposed by Flanigen *et al.* (40) and generally accepted for the interpretation of the skeletal spectra of zeolites. Instead, the picture quite agrees with that arising from the work of van Santen *et al.* (37). Any oxygen atom in any tetrahedra-based SiO_2 polymorph or zeolite is bonded rather symmetrically with two tetrahedral cations (T) giving rise to a bent T–O–T group. Assuming this group symmetrical and isolated, the site symmetry of oxygen is C_{2v}. So, the three degrees of freedom of any oxygen atom consist of two in-plane movements (A_1 and B_1) and one out-of-plane movement (B_2). The B_2 movement is associated to the out-of-plane deformation of the T–O–T group, the B_1 to the asymmetric stretching while the A_1 mode has both the character of a symmetric stretching and of an in-plane bending mode (scissoring). According to this, the three main IR bands observed in all silica polymorphs are classically assigned to the asymmetric stretching (arising from the A_1 mode, $\nu 1$), to the in-plane bending (arising from the B_1 mode, $\nu 2$) and to the out-of-plane "rocking" (arising from the B_2 mode, $\nu 3$) of the T–O–T groups. However, in this manner the movements of Si (or T) atoms are neglected, and the interpretation of the Raman spectra is difficult. On the other hand, if you take into account an isolated symmetric Si_2O molecule (C_{2v} point group) where Si atoms also are free to move, its total nine degrees of freedom (six of which arise from silicon and three from oxygen) constitute three translations, three rotations, and three vibrations. The three vibrations are the asymmetric stretching (B_1), the symmetric stretching (A_1) and the bending mode (A_1), while the B_2 mode became a rotation. So, if Si atoms are free to move, the in-plane motion of oxygen (A_1 symmetry), splits into two components, a bending mode ($\nu 2$) and a symmetric stretching mode ($\nu 4$). By analogy, by developing the central force network model of Sen and Thorpe (41), Galeener (39) showed that four main vibrational modes are expected for a tetrahedral silica network, i.e. a symmetric stretching, an antisymmetric stretching, a bending and a rocking mode. In the C_{2v} symmetry of T–O–T bent unities, the modes with A_1, B_1 and B_2 symmetry are both IR and Raman active. The strongest Raman mode, $\nu 4$, is assumed by Galeener (38) to be a symmetric stretching mode mainly because Raman peak intensity is generally greater for stretching than for bending modes. However, the coupling of this mode with the scissoring mode allows to explain the low frequency of the strongest Raman peak (550–350 cm^{-1}) in all silica polymorphs. On the other hand, it is clear that in the solid state to obtain that all T–O bonds expand in-phase, you need that simultaneously most T–O–T angles must contract. This mode is consequently highly sensitive to the structure of the polymorph, as indeed observed. The position of the strongest Raman peak, $\nu 4$, in fact, strongly depends on the type of rings present in silicas and silicates, as shown by Sharma *et al.* (42), and on the density of the unit cell, as shown by Kingma and Hemley for silicas (34). The position of the strongest Raman peak, $\nu 4$, in silicalite (380, 365 cm^{-1}) perfectly corresponds with the presence of five-membered rings and with its smallest density among silica polymorphs (1.76 g/cm^3 (1)), associated to its zeolitic nature.

As for the IR spectrum, the strongest complex band is $\nu 1$, observed in the 1300–950 cm^{-1} region and is associated to the asymmetric stretching of the T–O–T bridges. However, as recently pointed out by Kamitsos *et al.* (35), this mode is split into two components even in the case of vitreous silica, due to either the in-phase ($\nu 1'$) or the out-of-phase coupling ($\nu 1''$) of the asymmetric stretching modes of nearest T–O–T groups. In other words, this mode somewhat couples with the symmetric and asymmetric stretching of the four Si–O bonds of the SiO_4 octahedra. As shown in Table 2, it seems clear that the position of both $\nu 1'$ and $\nu 1''$ components is also somewhat sensitive to the size of the rings and/or to the density of the different silica polymorphs. This is particularly true for $\nu 1''$, whose shift is stronger, and that is actually resolved from $\nu 1'$ only in some cases, like just in the silicalite spectrum. In fact, the extent of the $\nu 1'$–$\nu 1''$ splitting and/or the position of the $\nu 1''$ mode near 1220 cm^{-1} have been considered to be indicative of the presence of 5-membered rings, like in the case of silicalite and the zeolites of the MFI family (2).

The $\nu 1$ modes are detectable nearly in the same position also in the Raman spectra but are very weak there because of the small change in polarizability of T–O–T bonds during the asymmetric stretching, if the two T atoms are equal.

As discussed above, the $\nu 2$ mode is essentially a bending mode of the T–O–T bridges, although mixed with a symmetric stretching mode, as assumed by Flanigen *et al.* (40). Its assignment predominantly to a bending mode is mainly due to its weakness in the Raman spectra, although its position is more typical of a symmetric stretching mode.

This mode appears to be the least sensitive to the structure, although is some cases it splits definitely in more components, like in the case of α-quartz where three well-resolved sharp bands are found.

The lowest frequency IR mode $\nu 3$ is associated to the out-of-plane deformation of the T–O–T bridges, so being a "rocking" mode. This explains why this mode is essentially silent in the Raman spectrum, while being very strong in IR in the region 430–490 cm^{-1} in all silica forms as well as in zeolites (17, 40).

As remarked above, besides the four vibrational modes discussed here and common to all silica's and network silicates and silico-aluminates, other structure-sensitive features are frequently present. They are associated to splitting of these vibrational modes (bands above 350 cm^{-1}) or to torsional lattice modes (below 400 cm^{-1}). A band near 550 cm^{-1}, like that observed in the silicalite spectrum, has been considered to be associated to the presence of fivefold rings (43). The ratio of the IR absorption in this region with respect to the absorption in the 450 cm^{-1} region has been used to determine the crystallinity of pentasyl MFI preparations (44, 45). In effect, the detection of this band is certainly useful as a test of crystallinity, as first proposed by Coudurier *et al.* (44), but is not strictly indicative of a five-membered ring structure. Other zeolites without 5-membered rings also show an IR band in a very near position (17, 40). The comparison with the spectra reported for cyclic siloxanes (46) and oligomeric silsesquioxanes (47) seem to indicate that a band in this region cannot be taken as a definite indication of a fivefold ring.

So, in our opinion, the detection of the $\nu 4$ mode near 380 cm^{-1} by Raman spectroscopy (385 cm^{-1} in the case of ZSM5 zeolite (48)) is the best tool for the spectroscopic identification of the MFI and similar structures, better than the detection of the IR mode near 550 cm^{-1}.

Both IR and Raman spectra of silicalite also show a weak band near 950 cm^{-1}. According to Scarano *et al.* (12) these features are associated to Si–(OH) stretching in hydrolyzed defects of the silicalite structure. In effect, our silicalite specimen presents a significant number of H-bonded silanols, evidenced by the band at 3510 cm^{-1} in the spectrum of outgassed pressed disks. This band is strong in the spectrum of our silicalite showing that our silicalite is rich in defects.

(*b*) *IR and Raman Spectra of Titanium-Silicalites and the Nature of Framework Titanium Sites*

As reported above the IR, Raman, and UV–vis spectra of the sample TS1E(1.25) show only and all the features expected for titanium silicalite, with evidence of negligible amounts of amorphous-like extraframework titanium or TiO_2 phases. Two main differences can be noted between the vibrational spectra of S1 and TS1: (i) a somewhat lower resolution of the TS1 spectrum; (ii) the detection of a medium intensity band centered in IR spectra near 950 cm^{-1} and in Raman spectra near 970 cm^{-1}.

The first difference could be partly related to the higher symmetry of TS1 (orthorombic) with respect to S1 (monoclinic), that tend to limit splittings and for which a smaller number of fundamentals is expected (see above).

As for the modes near 960 cm^{-1}, at least five different assignments have been proposed: (i) to the stretching of a titanyl group Ti=O (49); (ii) to the Ti–O stretching of TiO_4 tetrahedra (50); (iii) to the Si–O terminal stretching of Si–O...Ti bridges (51); (iv) to the terminal Si–O stretching of SiOH...(OH)Ti "defective sites" (12); (v) to the Si–O terminal stretching of "defects" still including the templating agent (52). Interestingly, Pilz *et al.* (9) argued that the Raman mode and the IR mode near 950 cm^{-1} should arise from two different vibrations, a Si–O stretching in IR and a Ti–O stretching in Raman. According to Boccuti *et al.* (51) and Scarano *et al.* (12) this band is sensitive to the presence of water and ammonia in both Raman and IR spectra, and should be due to contributions of both type (iii) and type (iv) modes. On the other hand, Bellussi *et al.* (53) showed that this band is not sensitive to H/D isotopic exchange, what should exclude type (iv) mode as the predominant one. Accordingly, this band has also been found in the spectra of amorphous silica containing Ti ions (25) that showed evidence of the presence of tetrahedrally bonded Ti cations (25, 53). This band has also been detected in the spectra of Ti-containing cristobalite (54).

Our spectra in the OH stretching region indicate that defects containing OH groups are by far less in our TS1 sample than in our S1 sample, at least in the conditions of our measurements, i.e., at the solid–vacuum interface. On the other hand IR spectra clearly show that the templating agent is not present in significant amounts. This seems sufficient to suppose that defects like those implied in the type (iv) and type (v) structures should not be predominant in producing this band.

According to our interpretation, this mode should arise from the asymmetric stretching mode of Si–O–Ti bridges ($\nu 1'$ mode), assuming Ti in a framework position. As discussed above, the mode $\nu 1'$ is intrinsically strong in IR but weak in Raman for silicas. The strength of the Raman peak for TS1 arises from the difference in polarizability of Ti–O and Si–O bonds, as well as to the intrinsically high Raman intensity of modes having an at least partial Ti–O stretching character. According to the centrosymmetry of the silicalite structure, obviously, the modes active in Raman are silent in IR and vice versa. However, the $\nu 1 - \nu 4$ modes discussed above are all split in a great number of components, some of which are IR active and other Raman active, due to crystal effect. So, in contrast to the Pilz *et al.* (9) arguments, the modes detected near 960 cm^{-1}

in the IR and Raman spectra of titanium silicalite should arise from IR active and Raman active components derived from the same $\nu 1'$ asymmetric stretching mode of Si–O–Ti bridges. Accordingly, they are detected at slightly different positions.

The shift down of this mode with respect to the position of the asymmetric stretching of Si–O–Si bridges is related to the greater weight of Ti with respect to Si and to the higher ionicity of Ti–O with respect to Si–O bonds. This interpretation is somewhat a "mixture" of the above type (ii) and type (iii) assignments, because it implies a mixing of Si–O and Ti–O stretching character. On the other hand, according to the above discussion, Si–O–Ti bridges should also give rise to shifts for the other modes. In effect, the subtraction IR spectra definitely show that a slight shift down is likely for the $\nu 1''$ and $\nu 2$ modes too. Moreover, a new IR component, evident as a shoulder in the TS1 spectra and giving rise to a rather strong band in the subtractions, can be found near 510 cm^{-1}. This mode is likely associated to the $\nu 3$ rocking mode, that is strong in IR. It seems reasonable that, if the stretching modes are shifted down by Ti for Si substitution, the rocking mode is shifted up. The other modes do not give rise to evident peaks either because they are weak (like $\nu 2$) or because they have a pronounced character of a framework vibration, like $\nu 4$.

This assignment does not contrast with that of Scarano *et al.* (12) because it is not excluded that Si–OH stretchings can have a minor role on it. Nevertheless, the perturbation of this mode in the presence of water and ammonia, as reported by Scarano *et al.* (12), does not necessarily implies a role of such hydrolyzed defects in the production of this band. In fact, these authors showed that this band is shifted upwards in Raman experiments in contact with ammonia and water. We have observed that this band is significantly shifted upwards when the templating agent is still present. This simply indicates that Ti ions interact with these molecules and that, upon this interaction, Ti–O bonds become less ionic, so more similar to Si–O bonds. This causes the Si–O–Ti asymmetric stretching mode to shift up, towards the position typical of Si–O–Si modes. This implies that Ti cations tend to expand their coordination from fourfold to fivefold or sixfold, that is the most usual overall coordination for Ti^{4+}.

In effect, the above presented data indicate that Lewis acidic Ti^{4+} cations actually exist in the TS1E(1.25) sample. On the other hand, in this sample Raman and UV spectroscopy exclude the presence of significant amounts of extraframework Titanium ions. Tetrahedral Ti^{4+} cations in the silicalite framework naturally tend to expand their overall coordination to octahedral, definitely preferred.

A similar behavior was also shown for tetrahedral Ti cations into amorphous silica, giving rise to stronger Lewis sites than octahedral Ti^{4+} cations exposed on TiO_2 surfaces (25, 55). Upon this interaction its coordination is expanded and the electron energy on them is increased. A similar interaction fully justifies the shift upwards of the Si–O–Ti asymmetric stretching mode described by Boccuti *et al.* (51) for the IR mode and Scarano *et al.* (12) for the Raman mode.

Raman and UV spectra show that the samples with excess Ti ions present extraframework Ti in the form of TiO_2-anatase. This phase is not detected by XRD likely because, due to its small particle size, their XRD peaks are very broad and masked by the sharp peaks of the MFI structures. It is less easily to explain why this phase is not evident in SEM micrographs and whether this phase has an adverse effect on phenol hydroxylation activity (as it would appear from the behaviour of the catalysts prepared with procedure 1) or not (as it could be concluded from the behaviour of catalysts prepared by procedure 2).

As remarked above, our samples show high catalytic activity in phenol hydroxylation, confirming that framework Ti cations are present and are active. However, in our case the 100% selectivity to cathechol at the expense of hydroquinone over the most active catalysts seems to be exceptional. According to some authors (56) an excess of cathechol among the products could be related to a blocking of pores, cathechol production occurring essentially at the external surface. Nevertheless, other authors disagree with this interpretation and argue that the reactions occur essentially inside the zeolitic pores (57). The composition of the reactant mixture (acetone to phenol ratio) and the TS1 crystal size have also a role in determining the ortho-vs-para slectivities. On the other hand, we found no hydroquinone on TS1E(1.25) that does not show any trace of the templating agent and only negligible traces of amorphous extraframework Ti species (see UV spectra), as well as on low-Ti-content samples of both TS1E and TS1T series. On the other hand, hydroquinone is found (although again in smaller amounts than usual) on the samples where extraframework TiO_2 is certainly present. It seems likely that this shift in selectivities is related to some details of our reaction conditions more than to the quality of the catalysts.

The maximum in catalytic activity for Ti contents 2.5% (TS1E series) or 5% (TS1T series), shown in Table 1, can be interpreted as the result of the increase of the activity associated to the slightly increasing amount of framework Ti^{4+} cations (see IR results) contrasted by the negative effect of the increasing amounts of extraframework TiO_2 in catalysing H_2O_2 decomposition.

CONCLUSIONS

From the present study we draw the following conclusions:

(i) By applying the preparation method described by Clerici *et al.* (15) we have prepared good silicalite and

titanium-silicalite samples, whose catalytic activity in phenol hydroxylation by H_2O_2 agrees with the literature data, although with a quite exceptionally high selectivity with respect to cathechol production. With Ti contents of 2.5 or above extraframework TiO_2 is certainly present in the form of anatase.

(ii) By applying a preparation method derived from those reported by Thangaraj *et al.* (16) we were unable to prepare pure titanium silicalite samples, being extraframework TiO_2-anatase detected already at 1.3% Ti content. On the other hand, also these samples proven to be active in phenol hydroxylation, with comparable activities and selectivities with respect to those obtained with procedure 1.

(iii) We developed an empirical assignment of most IR and Raman skeletal bands for these solids. From this we conclude that the most useful vibrational mode for the identification of MFI structures is the strongest Raman peak associated to a structure-sensitive symmetric stretching–bending mode of *T*–O–*T* bridges.

(iv) This model only partially agrees with the classical model used for the interpretation of the vibrational skeletal modes of zeolites, due to Flanigen and co-workers (40). The picture agrees well with that arises from the lattice dynamics calculations of van Santen *et al.* (37).

(v) From our model we assign the vibrational modes observed both in IR and in Raman spectra of TS1 near 960 cm^{-1} to different components arising from the asymmetric stretching mode of Si–O–Ti bridges.

(vi) we identified another mode typical of Si–O–Ti bridges of titanium silicalite, the rocking mode at 510 cm^{-1} in the IR spectra.

(vii) we showed that Ti cations in the silicalite framework act as Lewis acid sites also at the solid–gas interface, by coordinating ammonia, so giving rise to an expansion of its overall coordination to fivefold or sixfold.

ACKNOWLEDGMENTS

The authors gratefully acknowledge Professor S. Suib (University of Connecticut, Storrs) for performing XRD analyses, Dr. F. Geobaldo (University of Turin) for recording UV–vis spectra and Professor M. E. Davis (California Institute of Technology) and Dr. B. Notari for helpful suggestions.

REFERENCES

1. Flanigen, E. M., Bennett, J. M., Grose, R. W., Cohen, J. P., Patton, R. L., Kirchner, R. M., and Smith, J. V., *Nature* **271,** 512 (1978).
2. Meier, W. M., and Olson, D. H., "Atlas of Zeolites Structure Types," 2nd ed. Butterworths, London, 1992.
3. Kokotailo, G. T., Lawton, S. L., Olson, D. H., and Meier, W. M., *Nature* **272,** 437 (1978).
4. Chang, C. D., "Hydrocarbons from Methanol," Dekker, New York, 1983.
5. Taramasso, M., Perego, G., and Notari, B., U.S. patent 4 410 501 (1983).
6. Esposito, A., Taramasso, M., Neri, C., and Buonomo, F., U.K. Patent 2 116 974 B (1985).
7. Roffia, P., Leofanti, G., Mantegazza, M., Padovan, M., Petrini, G., Tonti, S., and Gervasutti, P., *in* "New Developments in Selective Oxidation" (G. Centi and F. Trifiro', Eds.), p. 43. Elsevier, Amsterdam, 1990.
8. Bellussi, G., Carati, A., Clerici, M. G., and Esposito, A., in "Preparation of Catalysts V" (G. Poncelet *et al.*, Eds.), p. 421. 1991.
9. Pilz, W., Peuker, Ch, Tuan, V. A., Fricke, R., and Kosslick, H., *Ber. Bunseges Phys. Chem.* **97,** 1037 (1993).
10. Geobaldo, F., Bordiga, S., Zecchina, A., Giamello, E., Leofanti, G., and Petrini, G., *Catal. Lett.* **16,** 109 (1992).
11. Bordiga, S., Boscherini, F., Coluccia, S., Genoni, F., Lamberti, C., Leofanti, G., Marchese, L., Petrini, G., Vlaic, G., and Zecchina, A., *Catal. Lett.* **26,** 195 (1994).
12. Scarano, D., Zecchina, A., Bordiga, S., Geobaldo, F., Spoto, G., Petrini, G., Leofanti, G., Padovan, M., and Tozzola, G., *J. Chem. Soc. Faraday Trans. I* **89,** 4123 (1993).
13. van der Pol, A. J. H. P., Verduyn, A. J., and van Hoof, J. H. C., *Appl. Catal.* **92,** 113 (1992).
14. Astorino, E., Master thesis, Northeastern University, Boston, 1994.
15. Clerici, M. G., Bellussi, G., and Romano, U., *J. Catal.* **129,** 159 (1991).
16. Thangaraj, A., Kumar, R., Mirajkar, S. P., and Ratnasamy, P., *J. Catal.* **130,** 1 (1991); Thangaraj, A., Eapen, M. J., Sivasanker, S., and Ratnasamy, P., *Zeolites* **12,** 943 (1992); Mirajkar, S. P., Thangaraj, A., and Shiralkar, V. P., *J. Phys. Chem.* **96,** 3073 (1992).
17. Szostak, R., Molecular Sieves, Principles of Synthesis and Identification, Van Nostrand Reinhold, New York, 1989.
18. Mentzen, B. F, and Sacerdote-Peronnet, M., *Mat. Res. Bull.* **28,** 1017 (1993).
19. Perego, G., Bellussi, G., Corno, C., Taramasso, M., Buonomo, F., and Esposito, A., in "New Development in Zeolite Science and Technology" (Y. Murakami, Eds.), p. 129. Elsevier, Amsterdam, 1986.
20. van der Pol, A. J. H. P., and van Hooff, J. H. C., *Appl. Catal. A Gen.* **92,** 93 (1992).
21. Zecchina, A., Bordiga, S., Spoto, G., Petrini, G., Leofanti, G., and Padovan, M., *J. Phys. Chem.* **96,** 4985 (1992).
22. Busca, G., Gallardo Amores, J. M., Piaggio, G., Ramis, G. and Sanchez Escribano, V., *J. Chem. Soc. Faraday Trans.* **90,** 3181 (1994).
23. Deo, G., Turek, A. M., Wachs, I. E., Huybrechts, D. R. C., and Jacobs, P. A., *Zeolites* **13,** 365 (1993).
24. Pilz, W., Peucher, Ch., Tuan, V. A., Fricke, R., and Kosslick, H., *Ber. Bunsen-Ges. Phys. Chem.* **97,** 1037 (1993).
25. Odenbrandt, C. U. I., Anderrsson, S. L. T., Andersson, L. A. H., Brandin, J. G. M., and Busca, G., *J. Catal.* **125,** 541 (1990); Li Yi, Ramis, G., Busca, G., and Lorenzelli, V., *J. Mater. Chem.* **4,** 1755 (1994).
26. Dessau, R. M., Schmitt, K. D., Kerr, G. T., Woolery, G. L. and Alemany, L. B., *J. Catal.* **104,** 484 (1987).
27. Zecchina, A., Bordiga, S., Spoto, G., Marchese, L., Petrini, G., Leofanti, G., and Padovan M., *J. Phys. Chem.* **96,** 4991 (1992).
28. Peri, J. B., *in* "Characterization and Catalyst Development" (S. A. Bradley, *et al.*, Eds.), p. 122. American Chem. Soc., Washington, 1989.
29. Bratos, S., and Ratajczak, H., *J. Chem. Phys.* **76,** 77 (1982).
30. Kiselev, A. V., Lygin, V. I., and Titova, T. I., *Zh. Fiz. Khim.* **38,** 2730 (1964).
31. Busca, G., Saussey, H., Saur, O., Lavalley, J. C., and Lorenzelli, V., *Appl. Catal.* **14,** 245 (1985).
32. Fateley, W. G., Dollish, F. R., McDevitt, N. T., and Bentley, F. F., "Infrared and Raman Selection Rules for Molecular and Lattice Vibrations," Wiley, New York, 1972.
33. Handke, M., and Mozgawa, W., *Vib. Spectrosc.* **5,** 75 (1993).
34. Kingma, K. J., and Hemley, R. J., *Amer. Mineral.* **79,** 269 (1994).

35. Kamitsos, E. I., Patsis, A. P., and Kordas, G., *Phys. Rev. B,* **48,** 12499 (1993).
36. Griffith, W. P., in "Spectroscopy of Inorganic-Based Materials" (R. J. H. Clark, and R. E. Hester, Eds.), Vol. 14, p. 119. Wiley, New York, 1987.
37. Van Santen, R. A., and Vogel, D. L., *Adv. Solid State Chem.* **1,** 151 (1989); deMan, A. J. M., van Beest, B. N. H., Leslie, M., and van Santen, R. A., *J. Phys. Chem.* **94,** 2524 (1990).
38. Bell, R. J., and Dean, P., *Deisc. Faraday Soc.* **50,** 55 (1970).
39. Galeener, F. L., *Phys. Rev. B* **19,** 4292 (1979).
40. Flanigen, E. M., *in* "Zeolite Chemistry and Catalysis" (J. A. Rabo, Ed.), p. 80. Amer. Chem. Soc., Washington, 1979.
41. Sen, P. N., and Thorpe, M. F., *Phys. Rev. B* **15,** 4030 (1977).
42. Sharma, S. K., Mammone, J. F., and Nicol, M. F., *Nature* **292,** 140 (1981).
43. Jacobs, P. A., Beyer, H. K., and Valyon, J., *Zeolites* **1,** 161 (1981).
44. Coudurier, G., Naccache, C., and Vedrine, J. C., *J. Chem. Soc. Chem. Commun.* 1413 (1982).
45. Shukla, D. B., and Pandya, V. P., *J. Chem. Technol. Biotechnol.* **44,** 147 (1989).
46. Griffiths, W. P. *J. Chem. Soc. B* 1372 (1969).
47. Voronkov, M. G., and Lavrentyev, V. I., "Topics in Current Chemistry" **102,** 1199 (1982).
48. Dutta, P. K., Mohana Rao, K., and Park, J. Y., *J. Phys. Chem.* **95,** 6654 (1991).
49. Notari, B., in "Innovation in Zeolite Materials Science" (P. J. Grobet, Ed.), p. 413. Elsevier, Amsterdam, 1987.
50. Zecchina, A., Spoto, G., Bordiga, S., Padovan, M., Leofanti, G., and Petrini, G., in "Catalysis and Adsorption by Zeolites" (G. Ohlmann *et al.,* Eds.), p. 671. Elsevier, Amsterdam, 1991.
51. Boccuti, M. R., Rao, K. M., Zecchina, A., Leofanti, G., and Petrini, G., *in* "Structure and Reactivity of Surfaces" (C. Morterra *et al.,* Eds.), p. 133. Elsevier, Amsterdam, 1989.
52. Camblor, M. A., Corma, A., and Perez-Pariente, J., *J. Chem. Soc. Chem. Commun.* 557 (1993).
53. Bellussi, G., Carati, A., Clerici, M. G., Maddinelli, G., and Millini R., *J. Catal.* **133,** 220 (1992).
54. Varshal, B. G., Bobrov, A. V., Marvin, B. N., Iljuchin, V. V. and Belov, N. V., *Dokl. Akad. Nauk. SSSR* **216,** 374 (1974).
55. Odenbrandt, C. U. I., Brandin, J. G. M., and Busca, G., *J. Catal.* **135,** 505 (1992).
56. Tuel, A., Diab, J., Gelin, P., Dufaux, M., Dutel, J. F., and Ben Taarit, Y., *J. Mol. Catal.* **63,** 95 (1990).
57. Bellussi, G., *in* "New Developments in Selective Oxidation," (G. Centi and F. Trifirò, Eds.), p. 41. Elsevier, Amsterdam, 1990.